Relationship between Chain Length, Disorder, and Resistivity in Polypyrrole Films

Carlos Cesar Bof Bufon, Judith Vollmer, and Thomas Heinzel*

Lehrstuhl für Festkörperphysik, Heinrich-Heine-Universität Düsseldorf, 40225 Düsseldorf, Germany

Pamela Espindola, Hermann John, and Jürgen Heinze*

Institut für Physikalische Chemie, Albertstr. 21, 79104 Freiburg, Germany

Received: June 28, 2005; In Final Form: August 18, 2005

The effects of the polymerization temperature and of voltammetric cycling on the chain length and the resistivity of polypyrrole films are investigated. The studies provide further proof for the existence of at least two different types of polypyrrole, the so-called PPy I and PPy II. As the electropolymerization of conjugated systems in contrast to normal polymerization reactions is a fully activated process, the generation of these different types of PPy depends on experimental parameters such as temperature or formation potentials. UV−vis measurements demonstrate that PPy II comprises significantly shorter chains than PPy I (8−12 vs 32−64 units); moreover, film conductivity is found to increase with the fraction of PPy II. This fraction is changed via the polymerization temperature as well as by cyclic voltammetry, both of which can induce a metal−insulator transition. The counter-intuitive relationship between resistivity and chain length is interpreted in terms of disorder-dominated transport, in which the shorter chains of PPy II support the formation of delocalized electronic states, thereby increasing the localization length. Thus, our results are in agreement with recent broadband reflectivity measurements.

Introduction

Polypyrrole (PPy) has become one of the most studied conductive polymers in the past decade.[1] Characteristics such as low oxidation potential, solubility in water of the pyrrole monomers,[2,3] high conductivity at room temperature of σ(293K),[4−6] as well as stability of charged samples under ambient conditions, make PPy both commercially and scientifically interesting. Electronic devices such as batteries and supercapacitors[2,3] have been suggested as possible applications. PPy is typically synthesized electrochemically by galvanostatic (constant current),[7] potentiostatic,[8] or potentiodynamic[9] methods. Recent measurements[10] show that PPy films typically contain PPy I and PPy II, two variants of PPy that can be clearly distinguished phenomenologically, for example, in cyclic voltammetry (CV). It is also known that as the growth temperature decreases or low formation potentials are applied, more PPy II is formed. Until recently, however, it has not been clarified which quantitative structural differences exist between PPy I and PPy II.[10]

Some new insights about the formation of conducting polymers can be gained from an analysis of the mechanism of electrochemical polymerization. Two essential factors influence this process. First, the anodic oxidation leading to conducting polymers involves a reaction sequence in which each coupling step has to be activated by the potential-dependent generation of two reactive species. Second, the rate constants of the dimerization reactions of chainlike conjugated oligomers and of their coupling steps with the original starting monomer decrease with increasing chain length. Moreover, the rates of all these second-order reactions are a function of the concentration of the reacting species. These findings and additional experimental results prove that the electropolymerization mechanism of chainlike conjugated polymers does not involve a chain propagation process with successive coupling steps of the starting radical cation.[11] However, it must be concluded that the oligomerization in solution preferably occurs via consecutive "dimerization" steps leading from a dimer to a tetramer and then to an octamer (Scheme 1).[11−17] Additionally, in all cases where the reaction rates between different reactive oligomers and the starting monomer are similar, trimers and pentamers may be formed within the initial period of oligomerization as well. The reactivities of the generated oligomeric intermediates depend on their respective charging level. Consequently, the applied formation potential steers the chain length of the resulting product. Thus, low oxidation potentials produce "short" chain lengths due to the fact that the oxidation level of the intermediates is low and, consequently, their reactivities decrease. The same effect is induced by lowering the temperature, which lowers the rate constants of the second-order coupling reactions.

A further important point in understanding the formation and structure of conducting polymers concerns the existence and stability of charged σ-intermediates (Scheme 1). These intermediates are formed within each coupling step during polymerization.[12−17] Experimental results as well as theoretical considerations clearly show that the stability of these σ-intermediates increases as a function of chain length and the proton elimination leading back to a neutral chain becomes slower and slower.[18] The reason for this effect is that the acidity of proton-containing σ-intermediates decreases for longer chain lengths. The positive charges are stabilized in dependence on electronic factors such as the +I effect, delocalization of charges, and planarization of the chains. Finally, the polymerization stops at a point where the reactivity of σ-coupled chains is so low that no proton elimination occurs.

The σ-coupled chains are part of the polymer structure in the charged state. They slowly decay after discharging of the polymeric material and form again during the charging process.

10.1021/jp053516j CCC: $30.25
Published on Web 09/24/2005

SCHEME 1. Mechanistic Pathway during Electropolymerization

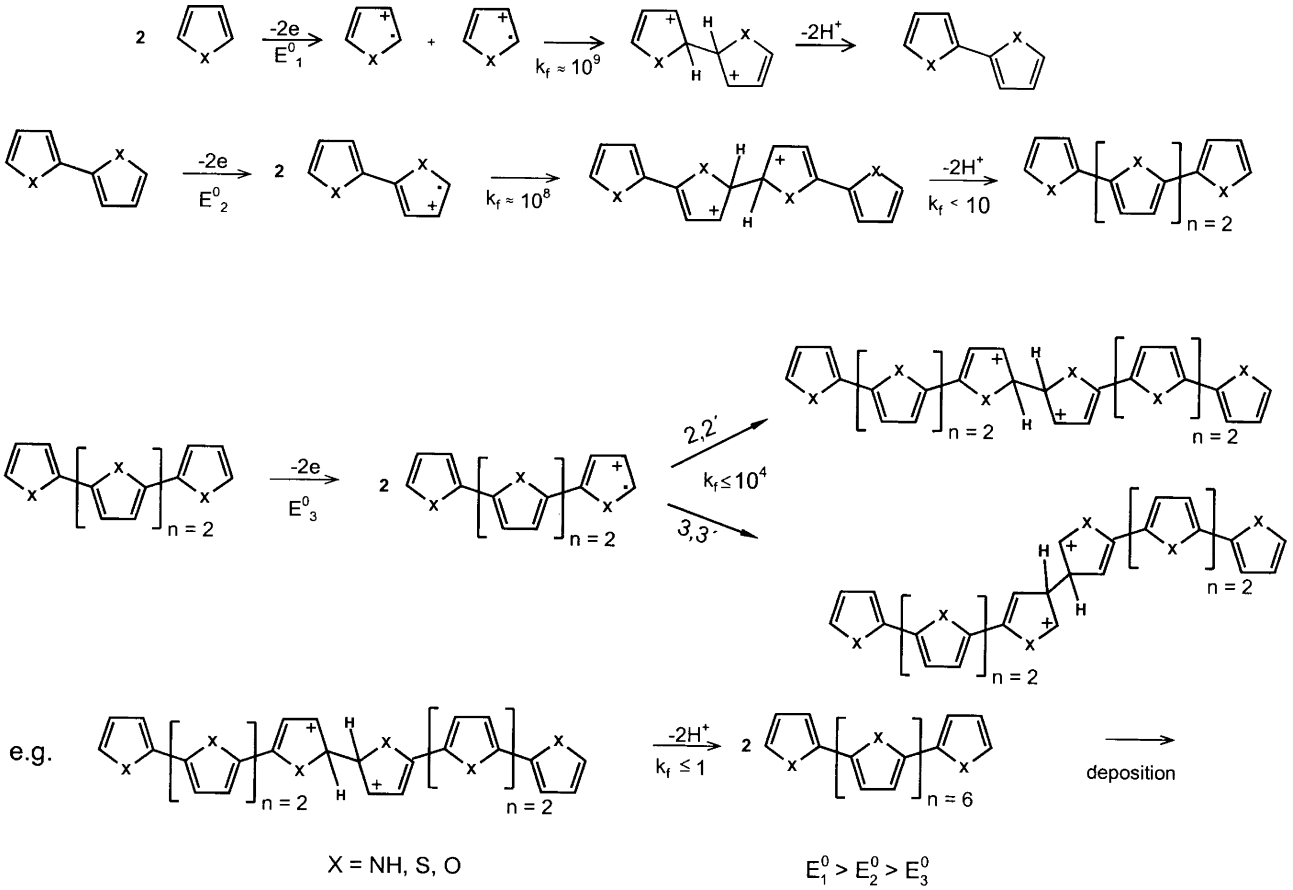

The formation of weakly interacting π-mers during the charging of conjugated oligomers and polymers has been discussed in the literature.[19−22] The unequivocal formation of σ-intermediates during the electropolymerization and their increasing stability for longer chains are compelling findings against the π hypothesis. Nevertheless, discussion on this topic has not yet been concluded.

A characteristic property of all chainlike conjugated systems is their conductivity which increases during charging. The charging of the films takes place simultaneously with the polymerization. Suitable anions that are added to the solution are deposited in the PPy film in this process. After synthesis, the charge density in the π-band apparently equals about one hole per three or four pyrrole units.[2]

To characterize and change the charge concentration of the polymer, CV in an electrolyte solution free of monomers is an established and powerful method.[1,23] The polymer chains are discharged during the reduction step, a process which is compensated by anions that drift out of the film and/or by the insertion of cations into the film, respectively.[10] The reverse processes occur during oxidation[24,25] which is sometimes referred to as p-doping of the polymer. The current−voltage curves for PF_6-doped PPy, performed during CV, exhibit a reduction wave at −0.28 V (vs Ag/AgCl) and an oxidation wave at 0 V.[10] It is well-known that CV induces a variety of further processes and effects. The formation of σ-bonds between chains during oxidation and their breakage during subsequent reduction steps have been discussed.[24] Furthermore, in situ conductivity measurements during CV show a characteristic hysteresis loop, indicating structural changes,[26] in particular, flattening of twisted chains as well as σ-bond formation[10,27] and intermolecular π-interaction.[28−30] Moreover, the volume and the mass of the films change as a function of the potential and the history of the film; finally, the cycling partly transforms PPy II into PPy I.[10,31]

Naturally, the mechanisms relevant for the electronic transport properties are of particular interest in conducting polymers. In the insulating phase of PPy, it is assumed that charge transport takes place via three-dimensional (3D) variable range hopping (VRH).[32] Another characteristic property of this phase is characterized by a positive magnetoresistivity, which increases roughly with the square of the magnetic field.[33−35] In the metallic phase, on the other hand, various models suggest a power law[34−36] or an exponential dependence[37] of the resistivity on the temperature. Here, a metal is usually defined as a system with a finite resistivity at zero temperature. In a recent series of experiments, the reflectivity of metallic PPy films has been studied over a wide range of frequencies.[38−40] These measurements strongly suggest that in the metallic regime, only a small fraction (a few percent at most) of the charge carriers participate in the conduction mechanism, while the majority of the charges is strongly localized. Several studies have reported a metal−insulator transition in PPy, which has been driven by varying the doping concentration,[33,41] the counterion type,[42] or the polymerization temperature.[36,43,44] Theoretical considerations imply that the two critical parameters for the metal−insulator transition are the interchain coupling strength and the disorder: As the system crosses from the insulating into the metallic phase, one-dimensional (1D) states (localized on a single chain) evolve into 3D states, which are delocalized over several chains with short-range order and form a bad metal.[45,46]

Hence, a lower polymerization temperature increases both the fraction of PPy II and its conductance and can even drive the films from the insulating into the metallic phase. This

phenomenological correlation raises the question we address below, namely, whether there is a causal dependence between the PPy II contents and the transport properties. We vary the fraction of PPy II in our films by two means, namely, by changing the polymerization temperature as well as by voltammetric cycling. From a combination of UV−vis spectroscopy with electronic transport measurements, at first sight, a surprising picture emerges: PPy II consists of oligomeric chains composed of eight monomers at most, while PPy I chains are significantly longer. Nevertheless, a larger fraction of PPy II increases the conductivity. We conclude that the chain length is of subordinate relevance for the resistivity but rather the short-range order as well as the interchain separation are most important.

Experimental Methods

Pyrrole (Aldrich) and acetonitrile (Riedel-de Haen) were distilled under argon atmosphere before the solution preparation. The synthesis solution was 0.5 M $TBAPF_6$, 0.5 M pyrrole, 1% distilled water, and 1% HCl. After composition, the solution was purged with argon for 20 min. The PPy films were grown galvanostatically in an electrochemical cell under argon overpressure.

PPy samples suited for UV−vis spectroscopy were polymerized in the synthesis solution, and the polymer was deposited on an indium tin oxide structure with an electroactive area of about 1.5 cm^2. The electrochemical experiments were carried out under argon atmosphere. A Pt net served as the counter electrode. The reference electrode was a Ag wire. An EG&G PARC Model 175 Universal programmer and a Jaissle potentiostat-galvanostat IMP 88 PC were used for electrochemical control and data recording. The UV−vis spectra were recorded on a Perkin-Elmer Lambda 9.

To force the formation of PPy I or PPy II, we had to vary the temperature and the current density. To obtain preferably PPy I, the electropolymerization was carried out at room temperature (293 K) using a current of 550 μA. To obtain mainly PPy II, electropolymerization took place at 243 K with a current of 100 μA. After polymerization, the films were reduced at a potential of −1.2 V and their UV−vis spectra were measured at room temperature.

For the preparation of films suited for resistivity studies, four platinum electrodes, patterned by microlithography, acted as a working electrode. The platinum contacts were deposited on top of a structure formed by a Si wafer doped with P and covered by a 100 nm SiO_2 layer, which generates a resistance between one platinum contact and the Si of typically 100 MΩ. The smallest separation between contacts is 2 μm. The electropolymerization was carried out at a current density of 6.6 mA/cm^2, applied for 30 s, which was supplied by a standard three-electrode potentiostast/galvanostat (Metrohm μu-Autolab). The synthesis solution was kept at temperatures of 293 and 273 K, respectively, within an accuracy of 0.1 K. Due to lateral growth, the films formed on the four working electrodes merged at a film thickness of about 4 μm, thus enabling electrical four-probe measurements. After polymerization, the samples were discharged (reduced) and recharged (oxidized) by CV in a monomer-free solution of 0.5 M $TBAPF_6$ in acetonitrile. The cycling was performed with a starting voltage of +1 V, a minimum voltage of −0.8 V (against Ag/AgCl), and a scan rate of 10 mV/s. To investigate the effect of the cycling on the transport properties, series of up to five samples grown from the same solution were exposed to a different number of complete cycles ending at $V = +1$ V. The samples were cleaned in distilled acetonitrile after cycling, to remove the residual $TBAPF_6$ on the surface, and dried at room temperature for one day in argon atmosphere.

The resistances are obtained by standard two- and four-terminal lock-in techniques, with an applied current of 100 nA at a frequency of 13.5 Hz. The film resistivity is obtained from the four-probe resistance after correction by a geometric factor. The frequency dependence of the impedance was measured at temperatures of 300 and 77 K, in a frequency range between 10 Hz and 100 kHz. The measurements as a function of temperature were carried out between 1.6 K and room temperature in an Oxford He^4 gas flow cryostat (1.6−90 K) equipped with a superconducting magnet (maximum field 8 T) and a Linkham nitrogen cryostat (85−300 K). Not all samples could be measured down to the lowest temperatures available, either because their resistance increased above the input impedance of the detection circuit (10 MΩ) or because leakage into the Si substrate became noticeable. Volume of the PPy films was determined from the lateral geometry, in combination with the measurement of the film thickness with an atomic force microscope.

Results

Electrochemical data and UV−vis spectra obtained at different temperatures give new insights into the structural differences between PPy I and PPy II. As can be seen in Figure 1a, the film produced at room temperature and high current shows the typical cyclic voltammogram of PPy I. The corresponding UV−vis spectrum of PPy I has an absorbance maximum at 426 nm and a shoulder at about 450 nm (Figure 1c). The cyclic voltammogram of the film prepared at lower temperature and lower current shows two oxidation peaks and one reduction peak (Figure 1b). The anodic peak at −0.12 V indicates the oxidation of PPy II, while that at a potential of +0.1 V corresponds to the oxidation of PPy I. These anodic peak potentials are not thermodynamic redox potentials; in particular, the anodic peak potential of PPy I is controlled by heterogeneous kinetics.[10] Considering the cyclic voltammogram, this film consists mainly of PPy II.

In the UV−vis spectrum of the same material after discharging, there is a broad absorbance maximum at about 386 nm for PPy II (Figure 1c). A second absorbance band in the range between 450 and 470 nm is caused by a small portion of PPy I. The molar extinction coefficient of the significantly longer PPy I chain is much higher than the extinction coefficient of PPy II due to the polarization of the long wavelength transition along the chain. Therefore, the signal caused by PPy I in the UV−vis spectrum can overlap the absorbance curve of PPy II and generates an additional broad absorbance maximum in the long wavelength range. In the given solvent/electrolyte system ($CH_3CN/(C_4H_9)_4NPF_6$), PPy II could not be obtained in pure form. Similar mild conditions in $PC/LiClO_4$ produce films of almost pure PPy II showing an absorption band at 380 nm (Figure 1d).

Zotti et al. have measured the electronic and electrochemical parameters of well-defined neutral oligopyrroles.[47] Parameters such as wavenumbers of polyconjugated polymers are known to linearly scale with the inverse of the degree of polymerization.[48] According to their results a longer polymer chain has an absorbance maximum at a lower wavenumber (longer wavelength) than a shorter polymer chain.

The number of pyrrole units N in a chain can be recalculated from the absorbance maximum by eq 1, the result of a linear regression of Figure 2

$$\nu = 22676\ \mathrm{cm}^{-1} + 25719\ \mathrm{cm}^{-1} \bullet (1/N) \qquad (1)$$

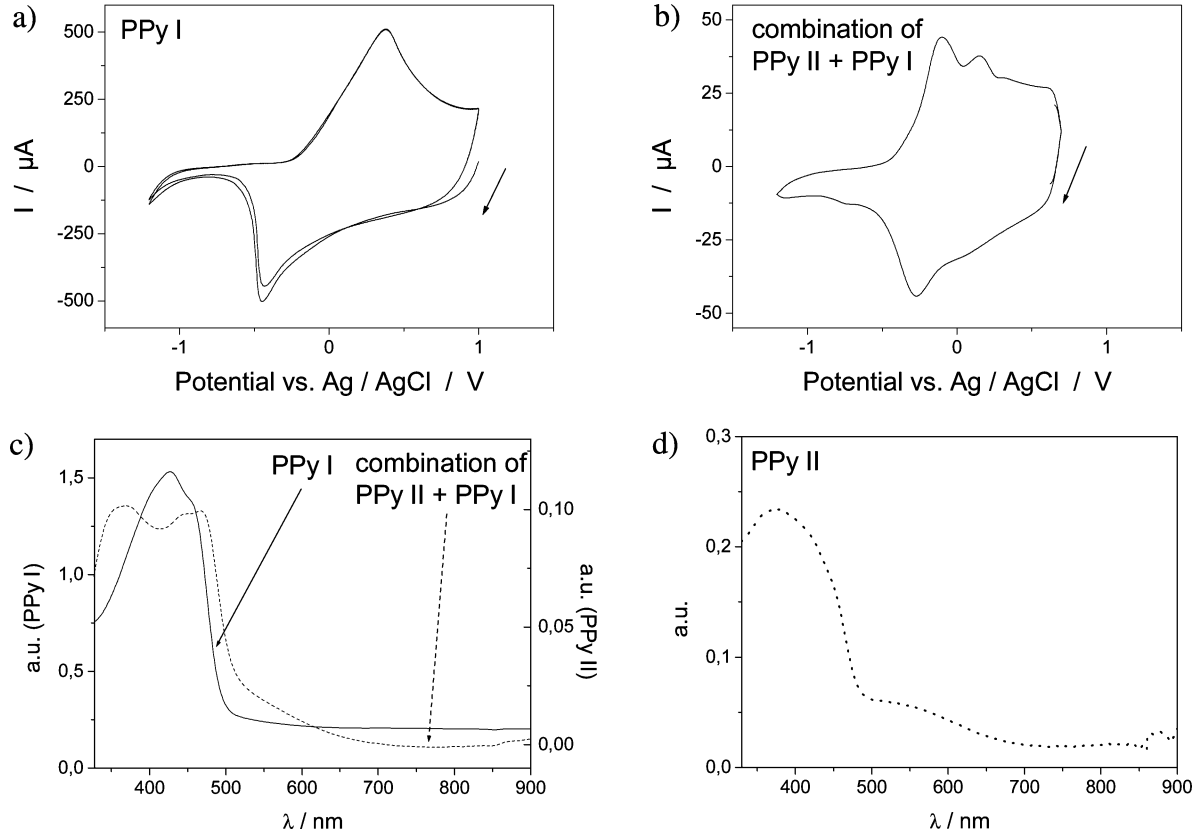

Figure 1. Cyclic voltammograms and UV−vis spectra of PPy films. Cyclic voltammograms after film deposition (0.02 V s^{-1}, monomer free cell). The films were galvanostatically polymerized under different conditions: (a) 550 μA, 3 min, 293 K (room temperature), $CH_3CN/(C_4H_9)_4NPF_6$, main product, PPy I (solid line in Figure 1c), (b) 100 μA, 3 min, 243 K, $CH_3CN/(C_4H_9)_4NPF_6$, main products, combination of PPy II + PPy I (dashed line in Figure 1c), (c) UV−vis spectra of PPy II and I at room temperature after reduction at a potential of −1.2 V ($CH_3CN/(C_4H_9)_4NPF_6$), solid line, pure PPy I, dashed line, combination of PPy II + PPy I, and (d) UV−vis spectra of PPy II at room temperature after reduction at a potential of −1.2 V ($PC/LiClO_4$), dotted line, pure PPy II.

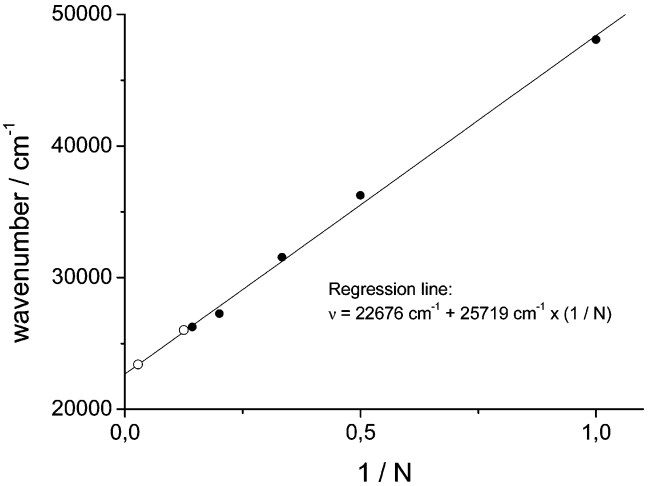

Figure 2. Correlation of wavenumbers vs 1/*N* (*N* = Number of pyrrole units for different oligopyrroles): correlation factor $r = 25\,719$, filled dots, Zotti et al.;[34] open dots, data from Figure 1.

Using eq 1, the number of pyrrole units of pure PPy I in the neutral state is about 32 ($\lambda_{max} = 426$ nm) to 64 and that of PPy II is 8 ($\lambda_{max} = 386$ nm) up to 12 ($\lambda_{max} = 403$ nm). Obviously, in the combination of both PPy components, PPy I contains longer chains (number of pyrrole units > 64, $\lambda_{max} = 450-470$ nm). It may be that the chains are cross-linked. It should be noted that a correlation between the wavelength and the number of units in the polypyrrole chain ends at a value of 440 nm. Therefore, the number of pyrrole units for longer chains is not precise.

Until now, the UV−vis spectra of the corresponding charged monomer and oligomeric pyrroles with the exception of PPy I and PPy II are not available due to the fact that these species are reactive and oligomerize in "fast" coupling steps at least up to PPy II. Therefore, a correlation between the number of pyrrole units *N* in a chain and the position of the absorbance maximum of a charged species is not posssible. However, it should be noted that the PPy chains during charging (oxidation) form "σ-dimers" which, in the case of α-coupling, double the chain length of the oligomer;[12−17] β-coupling cannot be excluded either.[49] Nevertheless, the conjugation length remains in the same range and leads to broader bands or shoulders. Each coupling step of charged oligomeric species leads to the formation of σ-intermediates during the polymerization process, the stability of which increases as a function of chain length. As long as the polymerization proceeds, the σ-intermediates eliminate protons, and neutral conjugated oligomers are generated which under the usual electrochemical galvanostatic conditions are at once charged again and form elongated σ-coupled intermediates. At the "end" of the polymerization, all these σ-products are stable in the charged state and decompose slowly after discharging, again forming neutral conjugated chains. It may be that these species are key materials for the description of the conductivity mechanisms in PPy films. As already mentioned, the chain lengths of the "polymers" become shorter when the temperature for electropolymerization is lowered. At low temperatures, the reactivities of the charged oligomers decrease and, consequently, the kinetics of coupling and proton elimination becomes slower leading to the formation of short oligomeric chains.

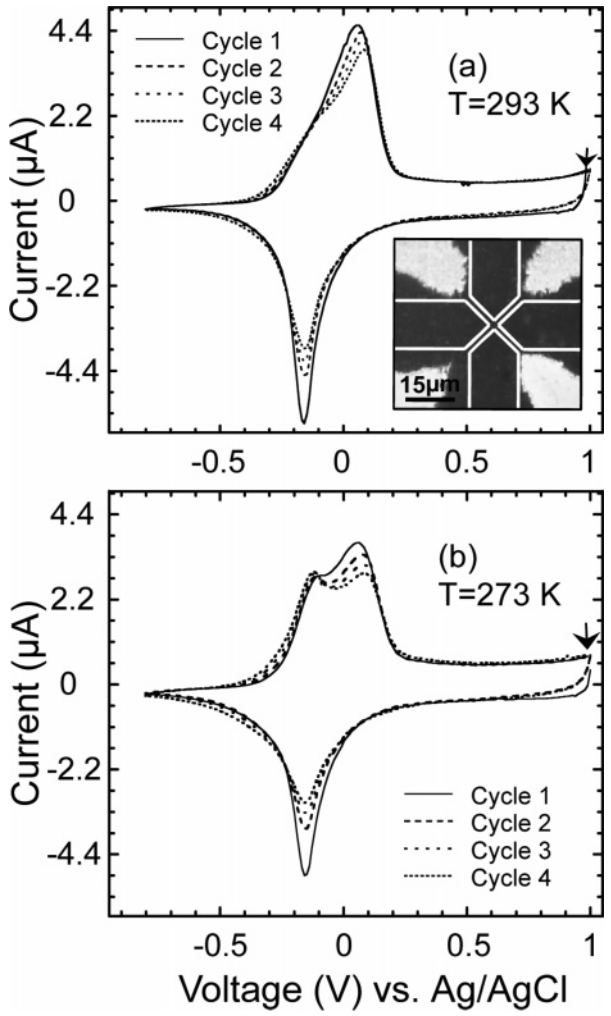

Figure 3. Current-to-voltage characteristics of four consecutive voltammetric cycles for samples grown at room temperature (a) and at 273 K (b). The arrow denotes the starting point. Inset shows the geometry of the PPy films (gray), as seen in an optical microscope. The edges of the Pt electrodes below the film are indicated by the white lines.

Normally, short monodisperse oligomeric chains form well-ordered structures on deposition.[50] Electrochemical quartz crystal microbalance studies of freshly polymerized PPy II films reveal an increase in mass of these films during repetitive redox switching.[10] This alteration occurs due to the incorporation of solvent and electrolyte into the polymer matrix. The result is an expansion of the polymer volume; therefore, distances increase between the polymer chains and the structural order decreases. Moreover, structural changes occur during repetitive cycling,[31] and PPy II is transformed into PPy I including a partial formation of a stable network.[10]

We proceed by discussing the influence of the polymerization temperature and of CV on the transport properties. Figure 3a shows the cyclic voltammogram of a sample grown at 293 K that underwent four cycles.

While the reduction peak appears at a constant voltage of −160 mV, a shift of the oxidation peak toward higher potentials is observed. We take this as an indication that during CV, PPy II is transformed into PPy I, in agreement with results reported earlier.[10] The presence of PPy II is also indicated by the shoulder in the oxidation peak at −150 mV. Furthermore, we observe a reduction of the peak amplitudes, which is most pronounced between the first and the second cycle. In the cycles higher than the first one, this apparent decay is usually attributed to the nonzero cycling speed, while the difference between the first two cycles again indicates a structural change in the polymer film, which will be of importance below. The voltammograms of samples grown at 273 K (b) show a more pronounced shoulder on the oxidation peak, indicating that the fraction of PPy II has increased. The PPy I oxidation peak again shifts to higher potentials as the number of cycles increases.

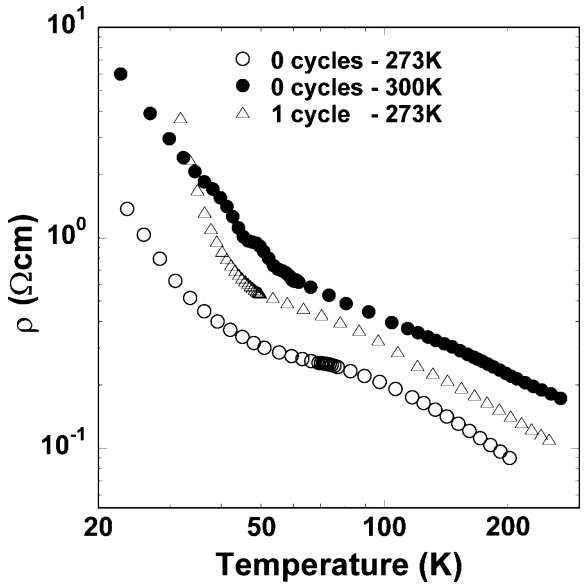

Figure 4. Resistivity for samples grown at 273 K remains below that of films grown at 293 K for all temperatures above 30 K, even after voltammetric cycling.

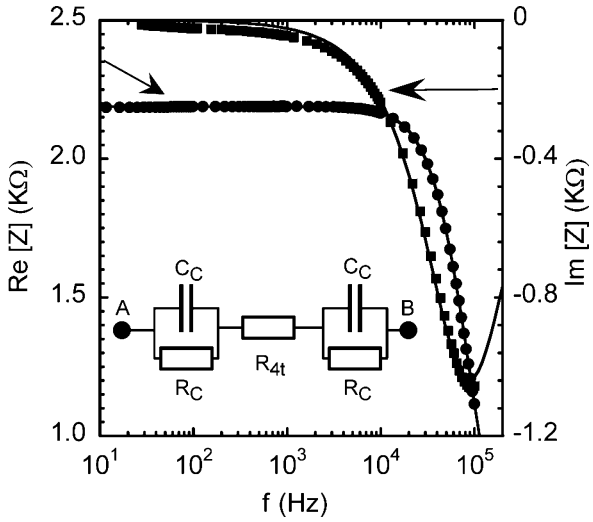

Figure 5. Frequency dependence of the real part (circles) and the imaginary part (squares) of $Z(f)$ at $T = 77$ K, as measured in a sample grown at 293 K that underwent a single voltammetric cycle. The lines are fits according to the equivalent circuit model (inset).

Samples grown at 273 K have significantly lower resistivities as compared to those grown at room temperature; see Figure 4. Voltammetric cycling increases the resistivity in all samples. However, even after several cycles, the resistivity of a sample polymerized at 273 K remains below that of the one prepared at 293 K that did not undergo CV. This indicates that changes in the growth temperature by 30 K have a stronger influence on the transport properties than CV.

Analyzing the frequency dependent capacitance $C(f)$ of the samples allows us to draw conclusions about the evolution of the density of mobile charges. In Figure 5 (a), a typical result for the impedance $Z(f)$ is reproduced. $Re(Z)$ drops markedly

around $f = 30$ kHz, while $Im(Z)$ shows a minimum around 80 kHz. These data are interpreted in terms of the equivalent circuit shown in the inset. In the experiment, the voltage of frequency f is applied between points A and B, while the current is detected at B. The two PPy−Pt contacts are modeled by equal contact resistances R_C and contact capacitances C_C, which are a consequence of the interface depletion layer.[51]

According to this model circuit, the frequency dependence of the impedance components given by

$$Re(Z(f)) = \frac{2R_C + {R_C}^2 R_{4t} \pi^2 f^2 {C_C}^2 + R_{4t}}{4{R_C}^2 \pi^2 f^2 {C_C}^2 + 1} \tag{2}$$

and

$$Im(Z(f)) = -\frac{{R_C}^2 \pi f C_C}{{R_C}^2 \pi^2 f^2 {C_C}^2 + {}^1/_4} \tag{3}$$

The resistance of the PPy film itself is R_{4t} and has been measured independently by four-terminal measurements, which do not show a frequency dependence. Thus, we obtain the capacitance and the resistance of the contacts by fitting the measurements to eqs 2 and 3, using R_C and C_C as fit parameters. The agreement is similar to that shown in Figure 5 for all samples.

We focus the contact capacitance C_C, which is relevant for our purpose. It depends neither on the number of cycles nor on the temperature and equals 1.7 ± 0.2 nF in all samples and at all temperatures. This indicates that the charge density on the polymer chains is independent of the number of cycles as well as of the temperature: Within the Schottky contact model,[51] the density of the charge carriers n in the semiconductor is given by

$$n = \frac{2V_{bi}{c_C}^2}{e\epsilon_0\epsilon_{PPy}} \tag{4}$$

Here, c_C denotes the contact capacitance per unit area, which equals 226 ± 25 nF/cm^2 in our samples, ϵ_{PPy} is the dielectric constant of the PPy film, and V_{bi} is built-in voltage between Pt and PPy. To estimate n, we use the literature value[52] for $\epsilon_{PPy} = 13.6$, while $V_{bi} \sim 1$ V has been reported[53] for metal−PPy contacts. A value of $n = (2.7 \pm 0.4) \times 10^{21}$ cm^{-3} at room temperature is found for all samples. These numbers are in rough agreement with the estimation of the charge deposited during oxidation, as obtained from integration of the oxidation trace of CV; see Figure 3. Here, a charge density of 2.6×10^{21} cm^{-3} is found for the first cycle, which decreases to 1.9×10^{21} cm^{-3} for the fourth cycle. We note that the carrier density n as obtained from this consideration is not necessarily equal to the density of carriers taking part in transport. Rather, it yields all carriers which become mobile in the strong electric fields present in the contact region. At the much weaker electric fields applied in the bulk, a large fraction of the charge carriers may remain immobile.

We proceed by discussing the effect of CV on the conductivity σ, which can be quite profound. In Figure 6a, the reduced activation energy, W, given by[35,54]

$$W = \frac{\mathrm{d} \ln \sigma(T)}{\mathrm{d} \ln T} \tag{5}$$

is shown for room-temperature grown samples which did not undergo CV (sample A), in comparison to a cycled one (sample B). For $\mathrm{d}W/\mathrm{d}T > 0$, the system is classified as a metal. For

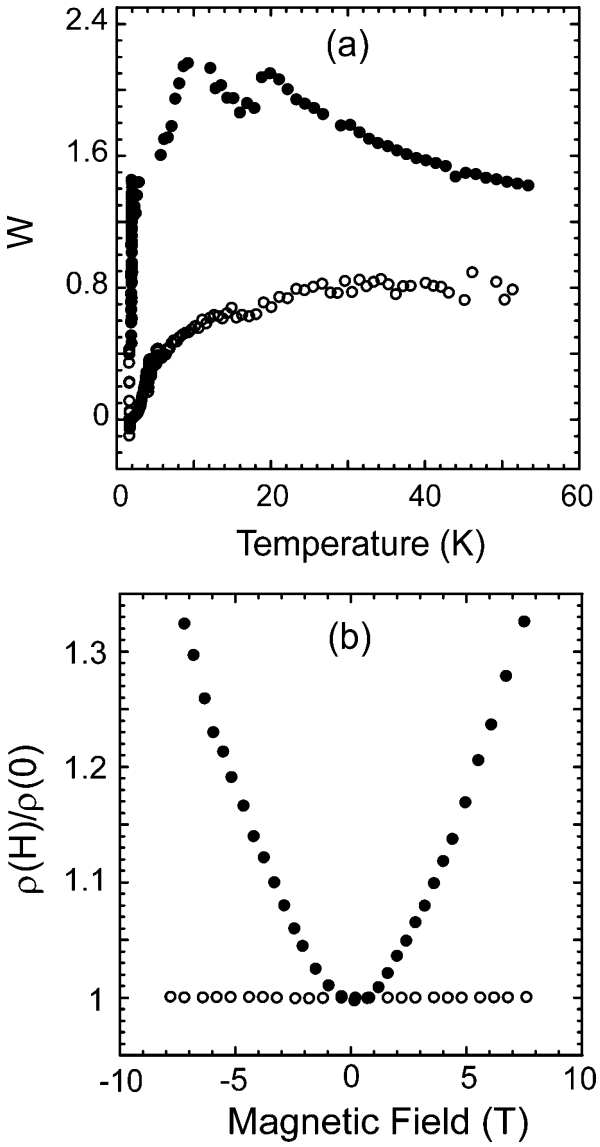

Figure 6. (a) Effect of the cycling on the temperature dependence of the reduced activation energy W as observed in an uncycled (open circles, sample A) and a cycled (full circles, sample B) PPy film. (b) The corresponding magnetoresistivities at $T = 2$ K with the magnetic field applied perpendicular to the film plane.

$\mathrm{d}W/\mathrm{d}T < 0$, the system is an insulator. In the uncycled sample, a positive slope indicates that PPy is in the metallic regime over the whole temperature range, except for $T < 1.9$ K, where a strong increase in W is observed. In the cycled sample, the slope is negative at more elevated temperatures, indicating an insulating regime. At temperatures below 10 K, this sample shows a metallic behavior as well. The low temperature anomalies are widely known and attributed to interference corrections,[37] which we do not consider here. Hence, the as-grown film is classified as a bad metal and is transformed into an insulator by a single voltammetric cycle. Further cycling does not change the insulating character.

This CV-driven metal−insulator transition also manifests itself in the magnetoresistivity $\rho(B)$ (Figure 6b). The resistivity of sample A shows no magnetic field dependence at 2 K, as expected for a carrier system with extended states, for example, within the Drude model.[55] Sample B, however, shows a strong, approximately parabolic magnetoresistance. At 8 T, ρ has increased by 30% compared to the value at $B = 0$. The origin of the parabolic magnetoresistance in strongly disordered media

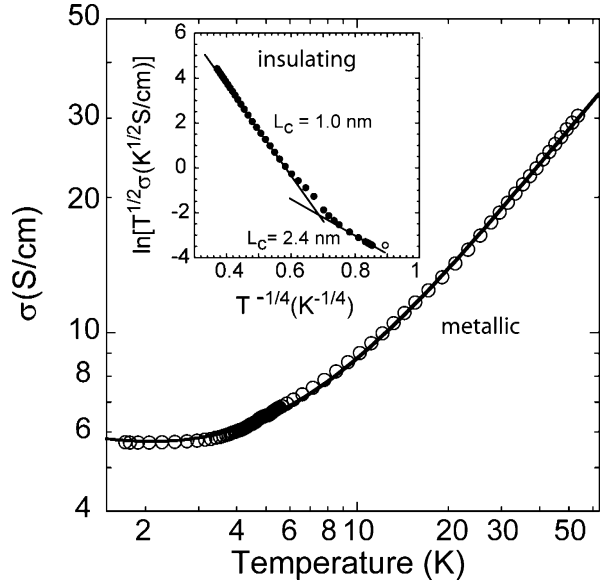

Figure 7. Fits of $\sigma(T)$ of Figure 6 in the metallic (main figure) and insulating (inset) regime. Data below 1.9 K have not been considered.

has been discussed elsewhere;[36] basically, within the VRH model, the magnetic confinement adds to the disorder potential and increases the tunnel barriers between the hopping sites.

From the transport measurements, we cannot clarify which of the processes that took place during CV (see Introduction) actually caused this transition. However, since the carrier density has remained constant, it is clear that the cycling increases the localization of the electronic states. We can extract the localization lengths by fitting the data to the models appropriate for the corresponding regimes; see Figure 7.

In the metallic regime, the temperature dependence can be modeled by a power law dependence

$$\sigma(T) = \sigma(0) + \alpha\sqrt{T} + \beta T^{p/2} \tag{6}$$

where the second term on the right-hand side originates from electron−electron interactions, while the third term takes localization effects into account.[37,56,57] A fit of the data to eq 6 with $\sigma(0)$, α, β, and p as fit parameters is shown in Figure 7. The exponent p is determined as $p = 1.02$. This is reasonable, since $p = 1$ has been predicted theoretically for systems close to the metal−insulator transition.[58] Moreover, a zero temperature conductivity of $\sigma(0) = 11.4$ S/cm is found. According to MacMillan[59]

$$\sigma(0) \approx 0.1\frac{e^2}{\hbar}1/L_C \tag{7}$$

which allows us to estimate the localization length in the metallic regime to $L_C = 21$ nm. This is a surprisingly large number considering the chain lengths of ∼12 nm for PPy I and ∼2.95 nm for PPy II (here, a length of one unit cell of a PPy chain containing two monomers of 0.735 nm has been assumed[60]). In the charged states, the chain lengths of "σ-dimers" should be considered. Consequently, the effective chain lengths of PPy I are expected to be 24 nm and those of PPy II 5.9 nm or even larger. It should be emphasized, though, that L_C is not a direct measure of the chain length but rather a characteristic length for the 3D extension of an electronic state that participates in transport. We conclude that the relevant electronic states in the metallic regime are extended over several chains.

The 3D VRH model[32,61] predicts a temperature-dependent conductivity in the insulating regime of

$$\sigma(T) = \frac{\sigma_0}{\sqrt{T}}\exp\left[-\left(\frac{T_0}{T}\right)^{1/4}\right] \tag{8}$$

Here, the characteristic temperature is given by

$$T_0 = \frac{16}{k_B D(E_F) L_c^{\,3}} \tag{9}$$

where $D(E_F)$ is the density of states at the Fermi level. To extract L_c, the density of states was assumed to be in agreement with the values reported for PPy in the literature,[34] that is, $D(E_F) = 5 \times 10^{20}$ eV^{-1} cm^{-3}. L_c can be determined by fitting the measurements to eq 8; see the inset in Figure 7. In the insulating samples at temperatures above 10 K, $L_c = 1.0$ nm is found. This indicates that after voltammetric cycling, the charges get localized on a length scale which corresponds to no more than three monomers. In addition, fits to the 1D VRH model are significantly worse, which we take as a signature that the hopping is 3D in character. Furthermore, we also fitted the data to an activated transport behavior, $\sigma(T) \propto \exp(E_a/k_BT)$, where E_a denotes the activation energy. These fits are significantly worse than those shown in Figure 7. This observation leads us to the conclusion that transport in the insulating regime does not take place by activation of localized carriers into empty, delocalized states, probably because such states no longer exist in the cycled sample.

Samples grown at 273 K are in the metallic state for temperatures above 40 K, while low-temperature anomalies are found at lower temperatures. Here, the metallic behavior could not be changed by CV, although the resistivity increased somewhat (Figure 4).

Interpretation and Discussion

Increasing the growth temperature as well as the first voltammetric cycle decreases the fraction of PPy II in PPy films. Simultaneously, the film resistivity increases. On the other hand, we have provided experimental evidence that PPy II consists of significantly shorter chains than PPy I, while the lengths of PPy I chains increase due to cyclic voltammetry. We, therefore, conclude that increasing the PPy chain length does *not* lead to an increase in the conductivity but rather some other mechanism is relevant. The observed increase in resistivity under voltammetric cycling can even go as far as to induce a metal−insulator transition, even though the carrier density is constant. We interpret these findings in terms of a disorder-dominated behavior. At lower polymerization temperatures, the reaction kinetics is slower, which results in shorter chains, but the film is given more time to form ordered structures, at least on a short range. This reduction of the disorder may be small in absolute terms but nevertheless relevant for the transport properties. Since, according to recent experimental results,[38−40] even in the metallic samples of the highest conductivities generated until now, at least 98% of the charge carriers are localized by disorder and do not contribute to the conductance: A small change in the degree of disorder can cause a dramatic difference in the density of delocalized carriers. The modifications that go along with a single voltammetric cycle can be sufficient to localize all carriers, thus driving the system from the metallic into the insulating phase.

Although we find a correlation between the PPy II contents and the conductivity, this does not necessarily mean that PPy

II generates an intrinsically better conducting film than PPy I. It should be emphasized that, beyond the characteristic length scale of localization, our transport measurements do not allow conclusions on the type of disorder introduced. In particular, it is not clear at all which of the mechanisms that takes place during voltammetric cycling is actually responsible for the increased localization. Mechanisms may even be dominant for the disorder which are not relevant for the PPy II to PPy I transformation, like, for example, the introduction of oxidative defects. However, the low oxidation potentials as well as the aprotic solvent applied in these studies exclude significant oxidative degradation processes. To give another example, it would be no contradiction to our results if under the conditions favorable for the formation of PPy II, a small amount of very long and highly conductive chains with low disorder were formed as well. To exclude such scenarios, it would be desirable to be able to study the microscopic structure of the films by complementary techniques and correlate them to a conductance on the length scale of individual chains. In particular, the evolution of the morphology of PPy films under cycling has recently been studied in situ by scanning probe techniques,[62] with the remarkable result that PPy II forms oriented fibrils with a characteristic size of 20−50 nm, while PPy I has a granular structure. When this result is taken into account, it is tempting to attribute the localization length in our metallic sample to the characteristic fibril size. It would thus be very interesting to perform similar in situ studies of the morphology of our films.

Summary and Conclusion

We have provided experimental evidence that PPy II consists of significantly shorter chains (8−12 units) as compared to PPy I (32 units), while at the same time films containing more PPy II show a larger conductivity. To explain these findings, we argue that increasing the PPy II fraction goes along with an increased localization length of the current carrying states, which is disorder driven. Such a mechanism would be in tune with the fact that the character of the current carrying states is 3D. A possible mechanism could be that the PPy II oligomers form a higher degree of short-range order than PPy I chains. We argue that the induced and presumably small changes in the disorder due to changes on the growth temperature or due to voltammetric cycling can have such a profound effect on the resistivity since, even in metallic samples, only a small fraction of the charge carriers resides in delocalized states. Our results thus support the conclusions drawn from recent broadband reflectivity measurements, which indicate that 98% or more of the carriers are localized even in the metallic regime. To further clarify the role of the different pyrrole oligomers in the transport properties of PPy films, it would be desirable to determine and control both the structure and the conductance on a microscopic scale.

Acknowledgment. Financial support by the DFG SFB 428, the Fonds der Chemischen Industrie, and by the Heinrich-Heine-Universität Düsseldorf is gratefully acknowledged.

References and Notes

(1) Skotheim, T. A.; Elsenbaumer, R. L.; Reynolds, J. R. *Handbook of Conducting Polymers*, 2nd ed.; Marcel Dekker: New York, 1998.

(2) Rodriguez, J.; Grande, H. J.; Cooper, T. F. In *Handbook of Organic Conductive Molecules and Polymers*; Nalwa, H. S., Ed.; John Wiley & Sons: New York, 1997.

(3) Simonet, J.; Berthelot, J. R. *Prog. Solid State Chem.* **1991**, *21*, 1.

(4) Ishiguro, T.; Kaneko, H.; Nogami, T.; Ishimoto, H.; Nishiyama, H.; Tsukamoto, J.; Takahashi, A.; Yamaura, M.; Hagiwara, T.; Sato, K. *Phys. Rev. Lett.* **1992**, *69*, 660.

(5) Sato, K.; Yamamura, M.; Hagiwara, T.; Murata, K.; Tokumoto, M. *Synth. Met.* **1991**, *40*, 35.

(6) Yamamura, M.; Hagiwara, T.; Iwata, K. *Synth. Met.* **1998**, *26*, 209.

(7) Lee, H. J.; Park, S. M. *J. Phys. Chem. B* **2004**, *108*, 1590.

(8) Ahmed, S. M.; Nagaoka, T.; Ogra, K. *Anal. Sci.* **1998**, *18*, 535.

(9) Zhou, M.; Heinze, J. *Electrochim. Acta* **1999**, *44*, 1733.

(10) Zhou, M.; Pagels, M.; Geschke, B.; Heinze, J. *J. Phys. Chem. B* **2002**, *106*, 10065.

(11) Smie, A.; Synowczyk, A.; Heinze, J.; Alle, R.; Tschuncky, P.; Götz, G.; Bäuerle, P. *J. Electroanal. Chem.* **1998**, *452*, 87.

(12) Smie, A.; Heinze, J. *Angew. Chem., Int. Ed. Engl.* **1997**, *36*, 363.

(13) Heinze, J.; Tschuncky, P.; Smie, A. *J. Solid State Electrochem.* **1998**, *2*, 102.

(14) Tschuncky, P.;. Heinze, J.; Smie, A.; Engelmann, G.; Koβmehl, G. *J. Electroanal. Chem.* **1997**, *433*, 223.

(15) Merz, A.; Kronberger, J.; Dunsch, L.; Neudeck, A.; Petr, A.; Parkanyi, L. *Angew. Chem.* **1999**, 111, 1533; *Angew. Chem., Int. Ed.* **1999**, *38*, 1442.

(16) Heinze, J.; Willman, C.; Bäuerle, P. *Angew. Chem., Int. Ed*. **2001**, *40*, 2861.

(17) Heinze, J.; John, H.; Dietrich, M.; Tschuncky, P. *Synth. Met.* **2001**, *119*, 49.

(18) Meerholz, K.; Heinze, J. *Electrochim. Acta* **1996**, *41*, 1839.

(19) Yu, Y.; Gunic, E.; Zinger, B.; Miller, L. L. *J. Am. Chem. Soc.* **1996**, *118*, 1013.

(20) Haare, J. A. E. H.; Groenendaal, L.; Havinga, E. E.; Janssen, R. A. J.; Meijer, E. E. *Angew. Chem., Int. Ed. Engl.* **1996**, *35*, 7638.

(21) Hapiot, P.; Audebert, P.; Monnier, K.; Pernaut, J.-M.; Garcia, P. *Chem. Mater.* **1994**, *6*, 1549.

(22) Aperloo, J. J.; Janssen, R. A. J.; Malenfant, P. R. L.; Groenendaal, L.; Fedet, J. N. J. *J. Am Chem. Soc.* **2000**, *122*, 7042.

(23) Heinze, J. *Top. Curr. Chem.* **1990**, *152*, 1.

(24) (a) Heinze, J. In *Organic Electrochemistry*; Lund, H., Hammerich, O., Eds.; Marcel Dekker: New York, 2001. (b) Heinze, J. In *Encyclopedia of Electrochemistry*; Bard, A. J., Stratmann, M., Schäfer, H. J., Eds.; Wiley-VCH: Weinheim, Germany, 2004; Vol. 8, pp 605−644.

(25) Levi, M. D.; Lopez, C.; Vieil, E.; Vorotyntsev, M. A. *Electrochim. Acta* **1997**, *42*, 757.

(26) Meerholz, K.; Heinze, J. *Synth. Met.* **1991**, 41−43, 2871.

(27) Pagels, M.; Heinze, J.; Geschke, B.; Rang, V. *Electrochim. Acta* **2001**, *46*, 3943.

(28) Zotti, G.; Berlin, A.; Pagani, G.; Schiavon, G.; Zecchin, S. *Adv. Mater.* **1993**, *6*, 231.

(29) Feldberg, S. W.; Rubinstein, J. R. *J. Electroanal. Chem.* **1989**, *240*, 1.

(30) Hill, M. G.; Pebbeau, J. F.; Zinger, B.; Mann, K. R.; Miller, L. L. *Chem. Mater.* **1992**, *4*, 1106.

(31) Levi, M. D.; Lankri, E.; Gofer, Y.; Aurbach, D.; Otero, T. *J. Electrochem. Soc.* **2002**, *149*, E204.

(32) Mott, N. F. *Metal Insulator Transitions*; Taylor and Francis: London, 1974.

(33) Sutar, D.; Mithra, M.; Menon, R.; Subramanyam; S. V. *Synth. Met.* **2001**, *119*, 455.

(34) Dugdale, J. *The Electrical Properties of Disordered Metals*; Cambridge University Press: Cambridge, U.K., 1995.

(35) Lee, P. A.; Ramakrishnan, T. V. *Rev. Mod. Phys.* **1985**, *57*, 287.

(36) Yoon, C. O.; Reghu, M.; Moses, D.; Heeger, A. J. *Phys. Rev. B* **1994**, *49*, 10851.

(37) Kaiser, A. B. *Rep. Prog. Phys.* **2001**, *64*, 1.

(38) Martens, H. C. F.; Brom, H. B.; Menon, R. *Phys. Rev. B* **2001**, *64*, 201102.

(39) Romijn, I. G.; Hupkes, H. J.; Martens, H. C. F.; Brom, H. B.; Mukherjee, A. K.; Menon, R. *Phys. Rev. Lett.* **2003**, *90*, 176602.

(40) Lee, K.; Heeger, A. J. *Phys. Rev. B* **2003**, *68*, 035201.

(41) Ishiguro, T.; Kaneko, H.; Nogami, Y.; Ishimoto, H.; Nishiyama, H.; Tsukamoto, J.; Takahashi, A.; Yamaura, M.; Hagiwara, T.; Sato, K. *Phys. Rev. Lett.* **1992**, *69*, 660.

(42) Ahlskog, M.; Mukherjee, A. K.; Menon, R. *Synth. Met.* **2001**, *119*, 457.

(43) Yoon, C. O.; Sung, H. K.; Kim, J. H.; Barsoukov, E.; Kim, J. H.; Lee, H. *Synth. Met.* **1999**, *99*, 201.

(44) Martens, H. C. F.; Brom, H. B.; Menon, R. *Phys. Rev. B* **2001**, *64*, 201102.

(45) Martens, H. C. F.; Brom, H. B. *Phys. Rev. B* **2004**, *70*, 241201.

(46) Prigodin, V. G.; Efetov, K. B. *Phys. Rev. Lett.* **1993**, *70*, 2932.

(47) Zotti, G.; Martina, S.; Wegner, G.; Schlüter, A.-D. *Adv. Mater.* **1992**, *4*, 798.

(48) Bredas, J. L.; Silbey, R.; Boudreaux, D. S.; Chance, R. R. *J. Am. Chem. Soc.* **1983**, *105*, 6555.

(49) Niziurski-Mann, R. E.; Scordilis-Kelley, C.; Liu, T.-E.; Cava, M. P.; Carlin, R. T. *J. Am. Chem. Soc.* **1993**, *115*, 887.

(50) Bäuerle, P.; Fischer, T.; Bidlingmaier, B.; Stabel, A.; Rabe, J. P. *Angew. Chem., Int. Ed. Engl.* **1995**, *34*, 303; *Angew. Chem.* **1995**, *107*, 335.
(51) Sze, S. M. *Physics of Semiconductor Devices*; John Wiley & Sons: New York, 1981.
(52) Koezuka, H.; Etoh, S. *J. Appl. Phys.* **1983**, *54*, 2511.
(53) Syed Abthagir, P.; Sarashwati, R. *J. Appl. Polym. Sci.* **2001**, *81*, 2127.
(54) Zabrodskii, A. G.; Zinoveva, K. N. *Sov. Phys. JETP* **1984**, *59*, 425.
(55) see, for example, Ashcroft, N. W.; Mermin, N. D. *Solid State Physics*; Holt Rinehart & Winston: New York, 2002.
(56) Altshuler, B. L.; Aronov, A. G. *Solid State Commun.* **1983**, *46*, 429.
(57) Mott, N. F.; Kaveh, M. *Adv. Phys.* **1985**, *34*, 329.
(58) Belitz, D.; Wysokinski, K. I. *Phys. Rev. B* **1987**, *36*, 9333.
(59) MacMillan, W. L. *Phys. Rev. B* **1981**, *24*, 2739.
(60) Geiss, R. H.; Street, G. B.; Volksen, W.; Economy, J. *IBM J. Res. Dev.* **1983**, *27*, 321.
(61) Joo, J.; Lee, J. K.; Lee, S. Y.; Jang, K. S.; Oh, E. J.; Epstein, A. J. *Macromolecules* **2000**, *33*, 5131.
(62) Cohen, Y. S.; Levi, M. D.; Aurbach, D. *Langmuir* **2003**, *19*, 9804.